

# New simulation technique to estimate the hydrocarbon type for the two untested members of Belayim Formation in the absence of pressure data, Badri Field, Gulf of Suez, Egypt

A. M. Abudeif<sup>1</sup>  · M. M. Attia<sup>1</sup> · A. E. Radwan<sup>2</sup>

Received: 2 February 2015 / Accepted: 10 September 2015 / Published online: 15 March 2016  
© Saudi Society for Geosciences 2016

**Abstract** Determination of the fluid type in a reservoir is considered one of the main essential purposes of the formation evaluation processes. Badri Field, located in the southern part of the Gulf of Suez, is one of the most prolific areas in the Gulf of Suez. Presence of sandstone streaks in Sidri and Baba members within Belayim Formation in some wells within this field of relatively high resistivity signature in electric logs is the main reason to investigate its petrophysical parameters, to delineate the main characterization of these sands, and to evaluate their ability for hydrocarbon accumulation and production. This study aims to estimate the fluid types in these two untested members, especially that they are sandwiched between two productive sandstone zones, Kareem Formation and Hammam Faraun Member. The fluid type can be determined using formation pressure and pressure gradient, which play a great role to differentiate between the different formations' fluids (oil, gas, and water). Because of absence of pressure data in the studied wells, a new simulation technique was applied using well logging crossplot responses in the different hydrocarbon types (oil and/or gas), which were tested before to estimate the fluid type in the untested two studied zones. These include density-neutron, sonic-neutron, *M-N*, and matrix identification (MID) crossplots. This can be performed by correlation of the crossplot responses in the two productive sandstone zones: Kareem Formation and Hammam Faraun Member versus the untested studied sandstone zones of Sidri and Baba members, depending on the similarities and the

differences between the crossplot responses or signatures in the oil and gas fluids. The results of this approach revealed that the most fluid type in BDR-A8 and BDR-B9 wells is gas in Baba and Sidri zones and oil in the BDR-A9 well for Baba zone.

**Keywords** Crossplots · Fluid types · Baba Member · Sidri Member · Badri Field · Gulf of Suez

## Introduction

Petroleum exploration around Gulf of Suez began just over 100 years ago at Ras Gemsa, with commercial scale of oil production starting in 1909. The Miocene sediments seem to have a very important role in oil accumulation in the Gulf of Suez. More detailed and comprehensive studies are needed to achieve a better understanding of the new promising areas, in which awaited detailed examination all over the Gulf of Suez should be performed. Alsharhan and Salah (1994) mentioned that “we must keep looking for stratigraphic traps in the southern Gulf of Suez.”

Analysis of pressure data is of prime interest for characterizing the multi-anomalous reservoirs. It can be used to differentiate between the different hydrocarbons (oil and/or gases) and water, in terms of their pressure gradients and slopes, when they have different pressure regimes. By systematically measuring the pressure points opposite each reservoir interval and then plotting them as a function of depth, the nature of fluids (gas, oil, or water) can be identified by studying the abrupt changes in the pressure gradients (Schlumberger 1986). All reservoir and production engineers are interested in knowing the fluid type which affect in their volumetric calculations and production facilities.

✉ A. M. Abudeif  
a\_abudeif@yahoo.com

<sup>1</sup> Geology Department, Faculty of Science, Sohag University, Sohag, Egypt

<sup>2</sup> Gulf of Suez Petroleum Company, Cairo, Egypt

Badri Field lies in the offshore part of the Gulf of Suez and covers an area of about 12 km<sup>2</sup>. It is located 625 m northeast of Morgan Field in the southern province of the Gulf of Suez, approximately 20 km northeast of Ras Shukheir area (Fig. 1). It is bounded by latitudes 33° 22' to 34° 47' N and longitudes 28° 24' to 28° 26' E.

Three wells only were chosen to perform the target of this work; these wells are BDR-A8 and BDR-A9 wells for Baba zone and BDR-B9 well for Sidri zone, where these wells have only three porosity logs (density, neutron, and sonic logs).

## Geologic setting

The Gulf of Suez is a Neogene continental rift system that developed by the separation of the African and Arabian plates in Late Oligocene-Early Miocene time. Geomorphologically, it represents a rejuvenated, slightly arcuate NW-SE topographic depression, known as the Clysmic Gulf. It extends northwestward from 27° 30' N to 30° 00' N. Its width varies from about 50 km at its northern end to about 90 km at its southern end where it merges with the Red Sea (El-Naby et al. 2010; Lashin and Abd El-Aal 2004; Bosworth and McClay 2001). The Gulf of Suez is dissected by a complex pattern of

faults: N-S to NNE-SSW as well as E-W-trending normal faults at the rift borders and within the rift basin, and NE-trending strike-slip faults crossing the Gulf basin (El-Naby et al. 2009). The interaction of these major fault systems resulted in a complex structural pattern consisting of numerous horsts and grabens with variable relief and dimensions. The Gulf of Suez is subdivided into three structural provinces according to their structural settings and regional dip directions: the northern Araba dip province (SW dips), the central Belayim dip province (NE dips), and the southern Amal-Zeit dip province (SW dips). These provinces are separated by two NE-trending accommodation zones: the Galala-Abu Zenima Accommodation Zone (GAZAZ) in the north and the Morgan Accommodation Zone (MAZ) in the south. Based on surface and subsurface data, the stratigraphic succession of the Gulf of Suez can be subdivided into three depositional units (Fig. 2) (El-Naby et al. 2009). The pre-rift units include Proterozoic basement rocks and Paleozoic to Upper Eocene sediments. These formations are important as source and reservoir rocks. The Upper Oligocene and Miocene syn-rift units contain source, reservoir, and seal lithologies, as well as volcanic rocks. The post-rift units are of Pliocene to Pleistocene age.

In terms of lithostratigraphy, Said (1990) mentioned that the stratigraphic sequence in the Gulf of Suez province is characterized by three depositional phases related to the Miocene rifting events. These are pre-rift phase (Early Paleozoic to Eocene), syn-rift phase (Early-Middle Miocene), and post-rift phase (Late Miocene and Pliocene). The syn-rift is characterized by its overall excellent qualities as source, reservoir, and seal rocks. The Belayim Formation is distinguished into four members, Hammam Faraun, Feiran, Sidri, and Baba. The clastic sands in Belayim Formation represent a good reservoir and have petroleum accumulation history especially in Hammam Faraun Member. The lithostratigraphic column for Miocene sediments in Badri Field is shown in Fig. 2.

## Material and methods

The goal of this study is to estimate the hydrocarbon type in the two untested zones of Sidri and Baba (S.S.) members in Badri Field. Schechter (2010) mentioned that crossplots are very important tools in formation evaluation processes. They help in determination of lithology and porosity of the formations. Crossplot techniques are affected by the reservoir minerals, shale contents, and gases.

This work will focus on the estimation of hydrocarbon type in the reservoir because it represents a problem in the formation evaluation processes of the two studied Sidri and Baba (S.S.) zones. A simulation technique was used between the crossplot responses of the well-logging (tested or produced) oil and gas fluids of Kareem and H. Faraun formations versus



**Fig. 1** Location map of the study area where the main Gulf of Suez oil fields are illustrated

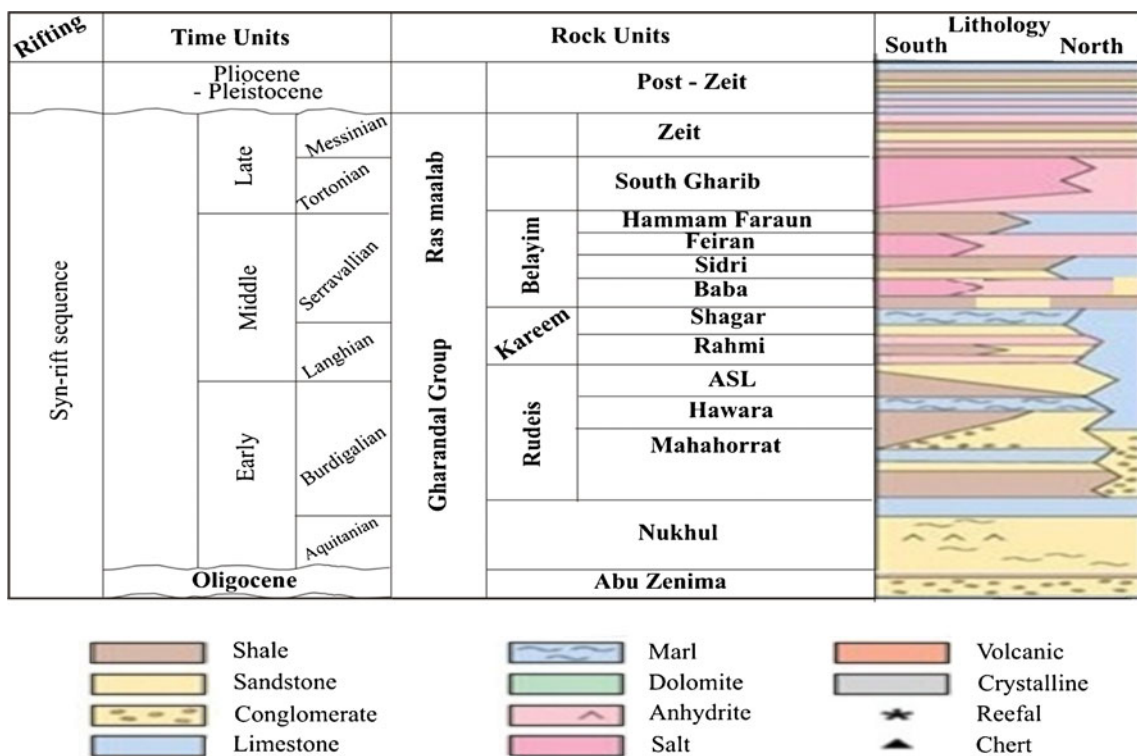


Fig. 2 Miocene stratigraphic column of Badri Field (modified after El-Naby et al. 2010; El-Naby et al. 2009; Schlumberger 1995)

the crossplot responses of the well-logging in the untested Sidri and Baba (S.S.) members. Density-neutron, sonic-neutron, *M-N*, and matrix identification (MID) crossplots were used in a systematic sequence.

*Hydrocarbon type estimation*

Determination of the hydrocarbon type in the reservoir is a very critical issue to geoscientists because it helps them understand the type of traps and their mechanism. Also, it helps production engineers make a decision about the production methods, completion pipe, and facilities. Finally, reservoir engineers are interested in the volumetric calculations of the hydrocarbons which differ in oil than in gas.

In general, the fluid type can be determined by using the formation pressure data and the pressure gradient, which play an important role to differentiate between the different formation fluids (oil, gas, and water). No pressure data was recorded in the studied wells, so this study depended only on the well logs relations. Asquith and Krygowski (2004) stated that determination of the fluid type which was contained within the pore spaces of the formation is achieved by observed relationships between the neutron and density logs. Also the deep resistivity reading is important to separate between water zone (low resistivity) and hydrocarbon zone (high resistivity). Gas zones will exhibit a greater density/neutron crossover than oil zones. Gas is most likely present if the magnitude of crossover increased, that is, the separation between the two curves is

pronounced while oil is inferred where the magnitude of crossover is low. Gas in the pores causes the density porosity to be too high (gas has a lower density than oil or water) and causes the neutron porosity to be too low (there is a lower concentration of hydrogen atoms in gas than in oil and water).

The determination of hydrocarbon type in the two studied zones needs a special petrophysical confirmation, in addition to the quick look method which was represented by the observed relationship between density and neutron curves, so the well logging crossplot technique was used to get more confirmation about the estimation of hydrocarbon type in the studied wells.

*Well logging crossplots*

Crossplots are a graphical solution to solve fairly complex relationships using two (or three) porosity measurements to estimate formation lithology and porosity. All these crossplots have the same general format: one measurement is displayed along the *x*-axis, and another is displayed along the *y*-axis. The measurements are either in porosity units referenced to limestone or, in the case of density and sonic logs, in the original measurement units ( $p_b$  in  $g/cm^3$  or  $kg/m^3$  for the density, and  $\Delta t$  in  $\mu s/ft$  or  $\mu s/m$  for the sonic). Superimposed on the plot (as an overlay) are pure lithology lines, usually sandstone, limestone, and dolomite. Porosity is indicated along each of these lines (Asquith and Krygowski 2004).

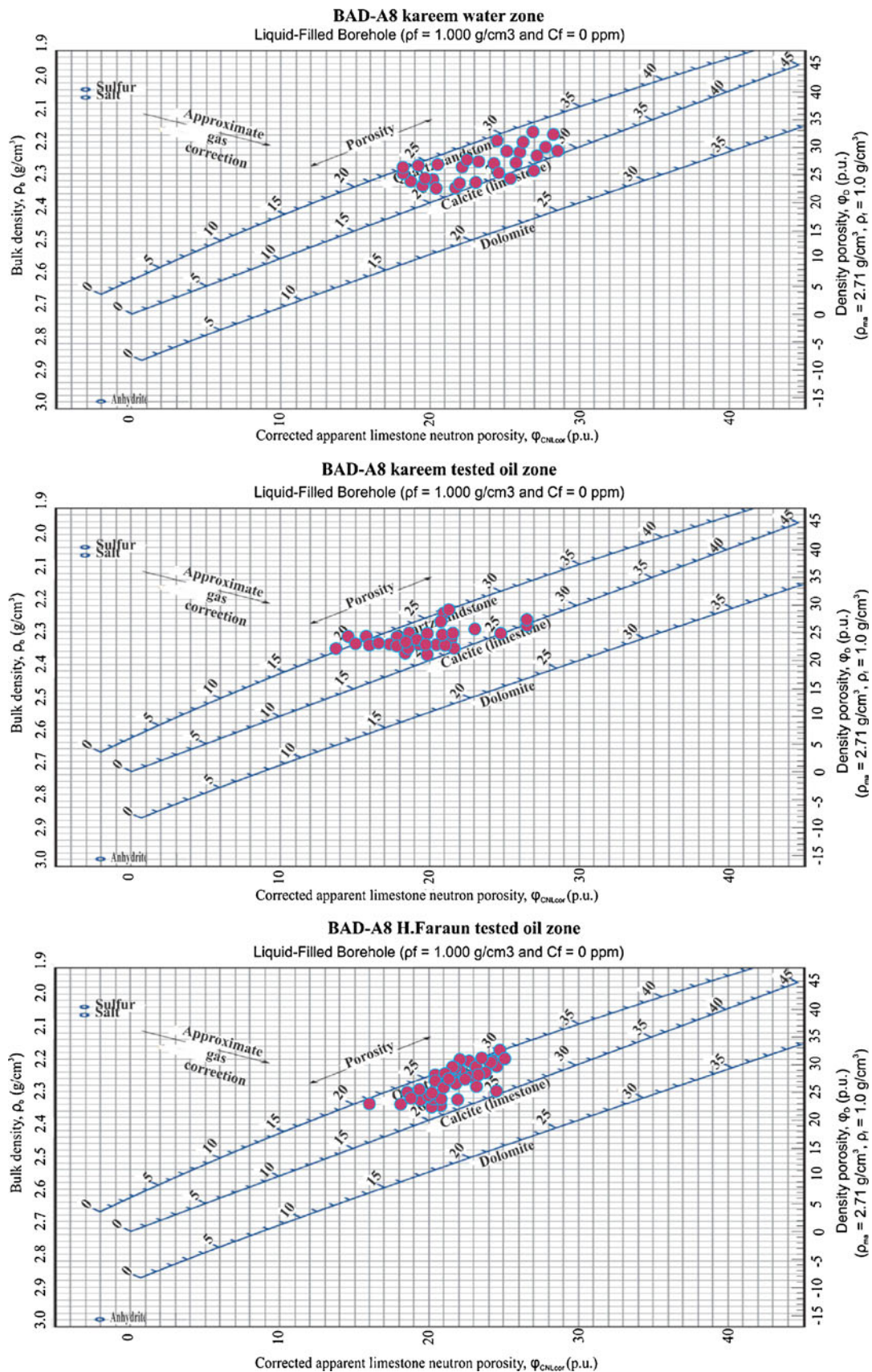


**Fig. 3** Density-neutron crossplots of H. Faraun and Kareem oil zones, and Kareem water zone for BDR-A8 well

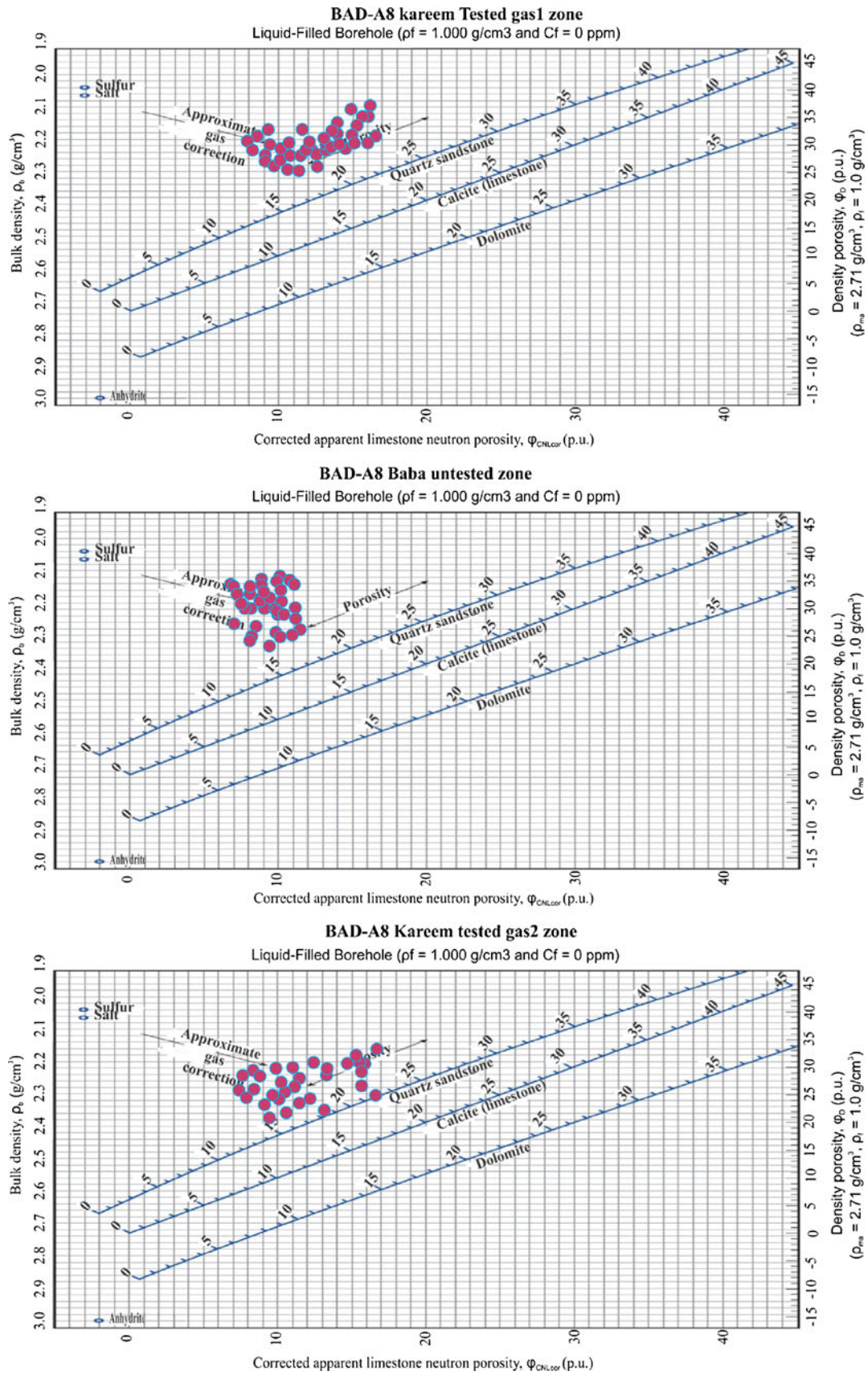


Fig. 4 Density-neutron crossplots of Kareem FM (gas 1 and gas 2 zones) and Baba S.S. zone for BDR-A8 well

Well logging crossplot is considered a special petrophysical study, and this study of a certain formation comprises various petrophysical analyses and tests away from the routine well logging analyses. These petrophysical studies are essential and reliable to get more realistic well logging values and a clear picture of the formation evaluation process. The petrophysical analyses that were done in this study are neutron-density, neutron-sonic, *M-N*, and *MID* crossplots based on the logs availability. Crossplots are important for establishing the lithology and mineralogy for any formation. These crossplots are sometimes two dimensional (of two log parameters), three dimensional (of three log

parameters termed *Z* plot) or a combination of all three porosity logs to provide the lithology characteristics (*M-N* plot). It is important to locate the position of the most probable presented minerals that are determined from all of these plots (Schlumberger 1987).

*Density-neutron crossplot*

The neutron-density crossplot can be used to differentiate between the common reservoir rocks [quartz sandstone, calcite (limestone), and dolomite], shale, and some evaporites which also can help for gas detection (Schlumberger 1997).

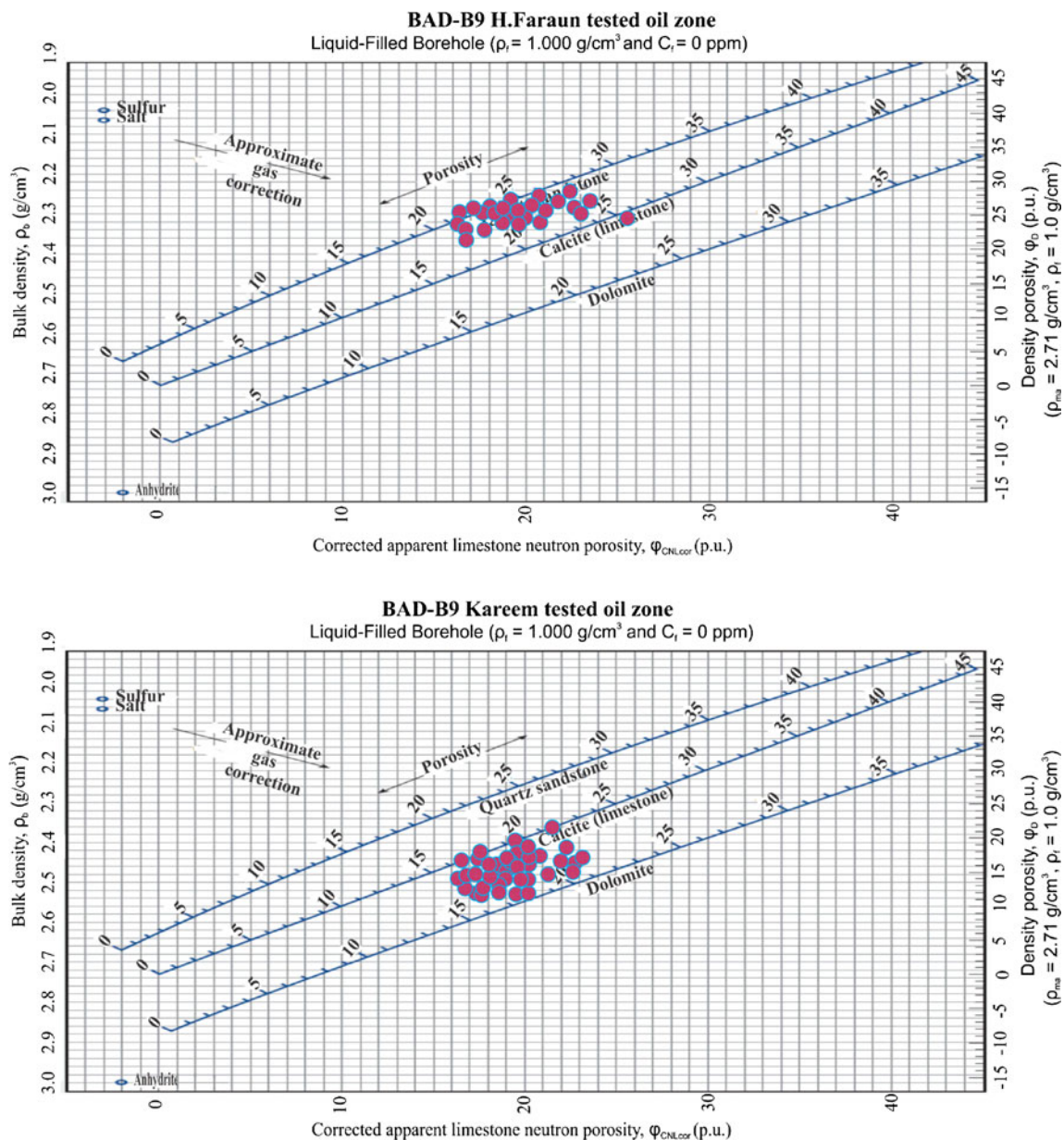


**Fig. 5** Density-neutron crossplots of Kareem and H. Faraun S.S. oil zones for BDR-B9 well

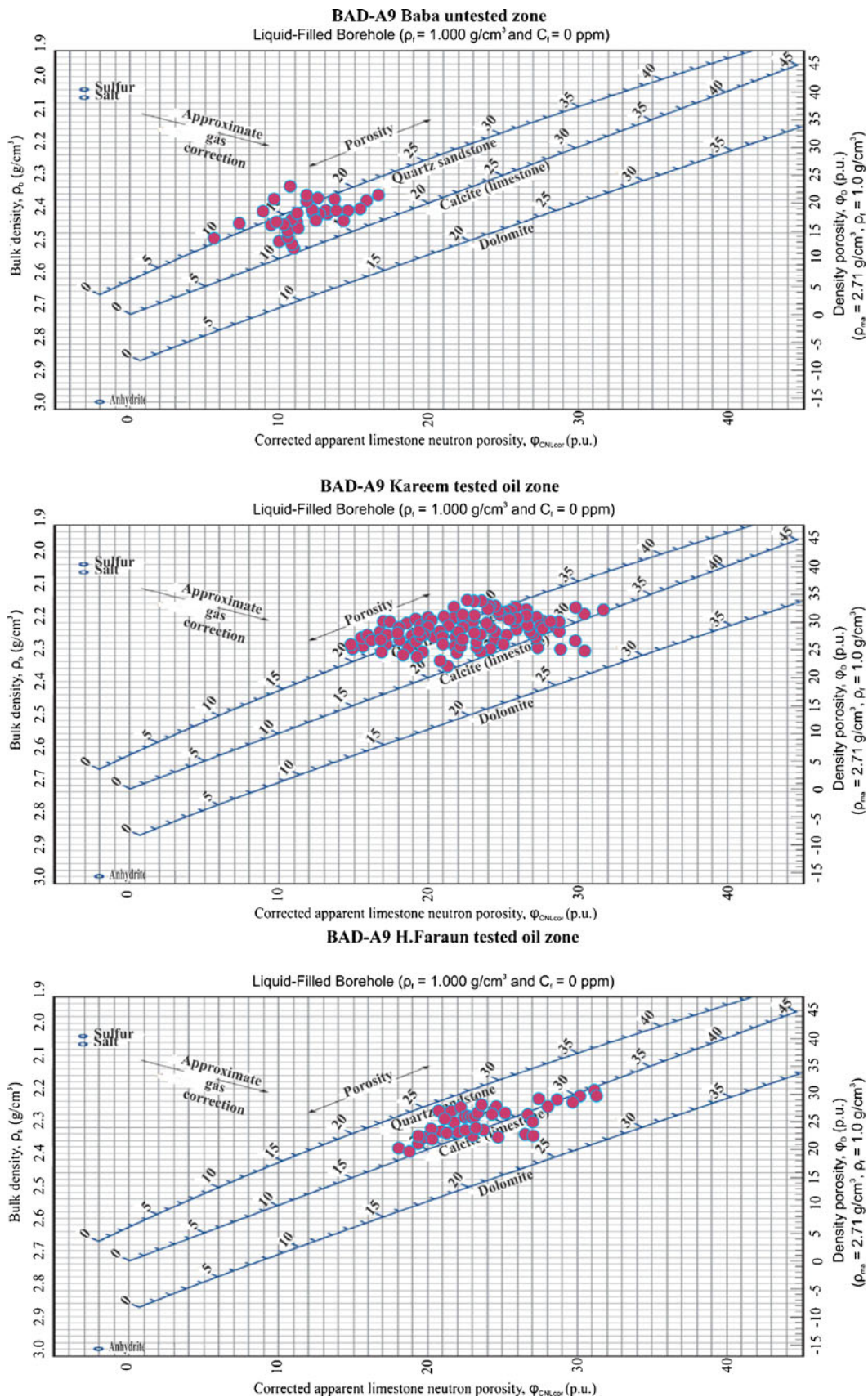


**Fig. 6** Density-neutron crossplots of H. Farau and Kareem oil zones, and Baba zone for BDR-A9 well

Sonic-neutron crossplot

The sonic-neutron crossplot can be used to differentiate between the common reservoir rocks when clay content is negligible. Sonic-density can be used to differentiate between a single known reservoir rock and shale and to identify evaporite minerals (Schlumberger 1997).

M-N crossplot

This technique depends on the fluid and log parameters which incorporate together essentially in the three porosity logs: sonic, density, and neutron. In complex lithology, the M-N

crossplot or tri-porosity crossplot is used to identify the mineral mixtures (Schlumberger 1997).

From the values of sonic, density, and neutron, two functions *M* and *N* are calculated, which are independent of primary porosity; therefore, a crossplot of these two quantities makes lithology characteristics more apparent. Two parameters independent of porosity are derived by the following equations (Pirson 1977):

$$M = \left[ (\Delta t_f - \Delta t_{log}) / (\rho_b - \rho_f) \right] * 0.01 \tag{1}$$

$$N = (\phi_{nf} - \phi_{nlog}) / (\rho_b - \rho_f) \tag{2}$$

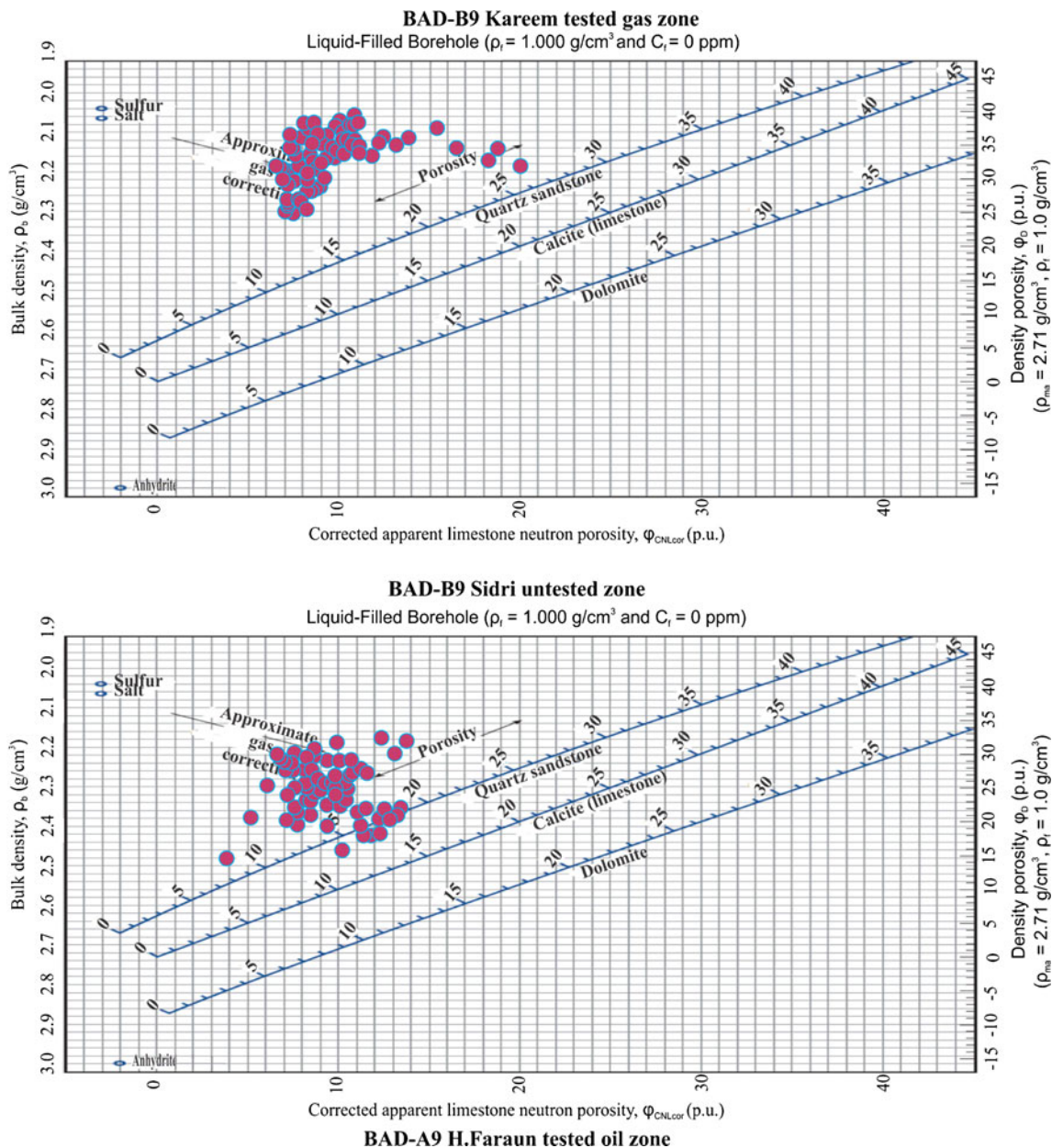
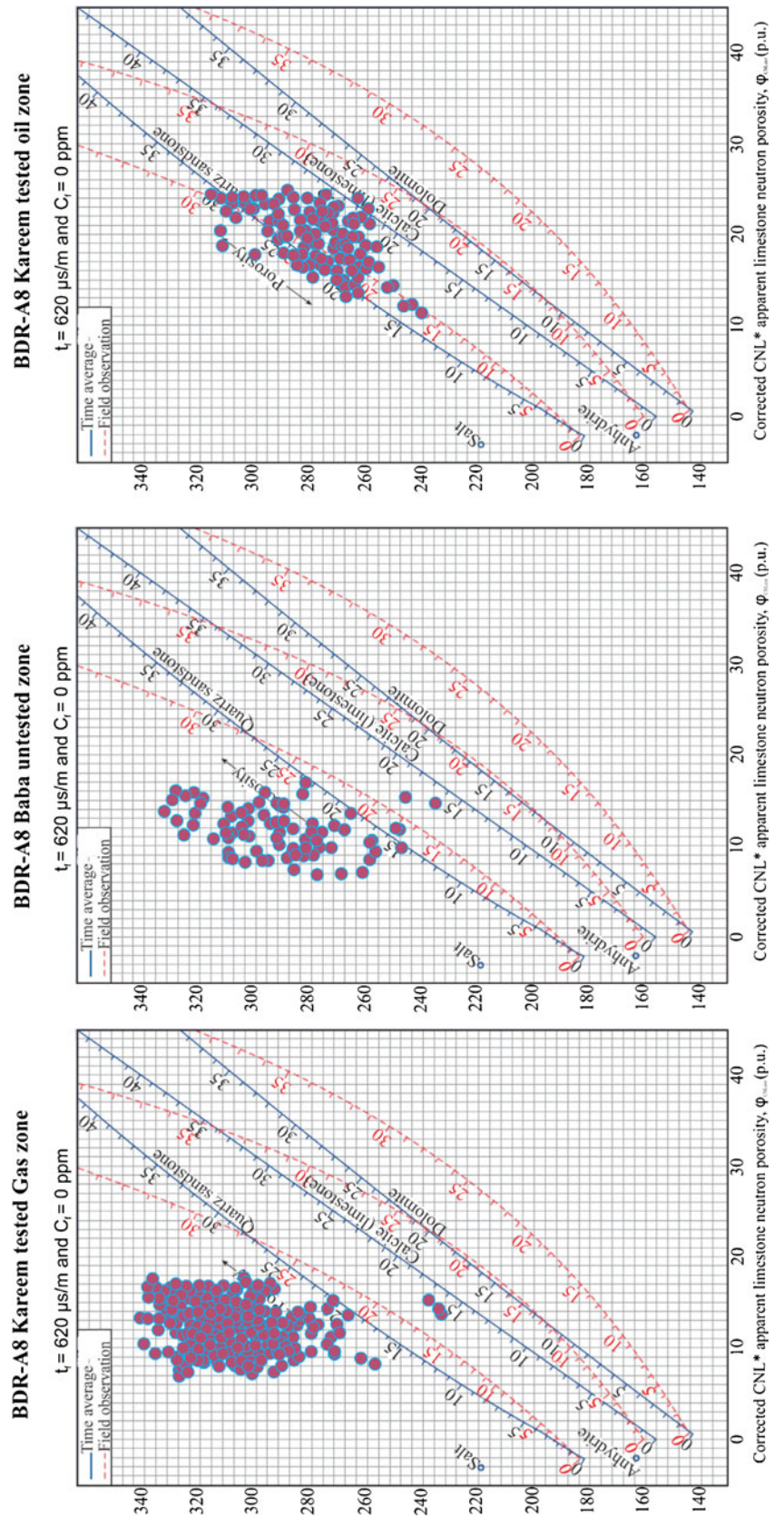


Fig. 7 Density-neutron crossplots of Kareem S.S. gas zone and Sidri S.S. zone for BDR-B9 well



**Fig. 8** Sonic-neutron crossplots of Kareem gas and oil zones and Baba sand zone for BDR-A8 well



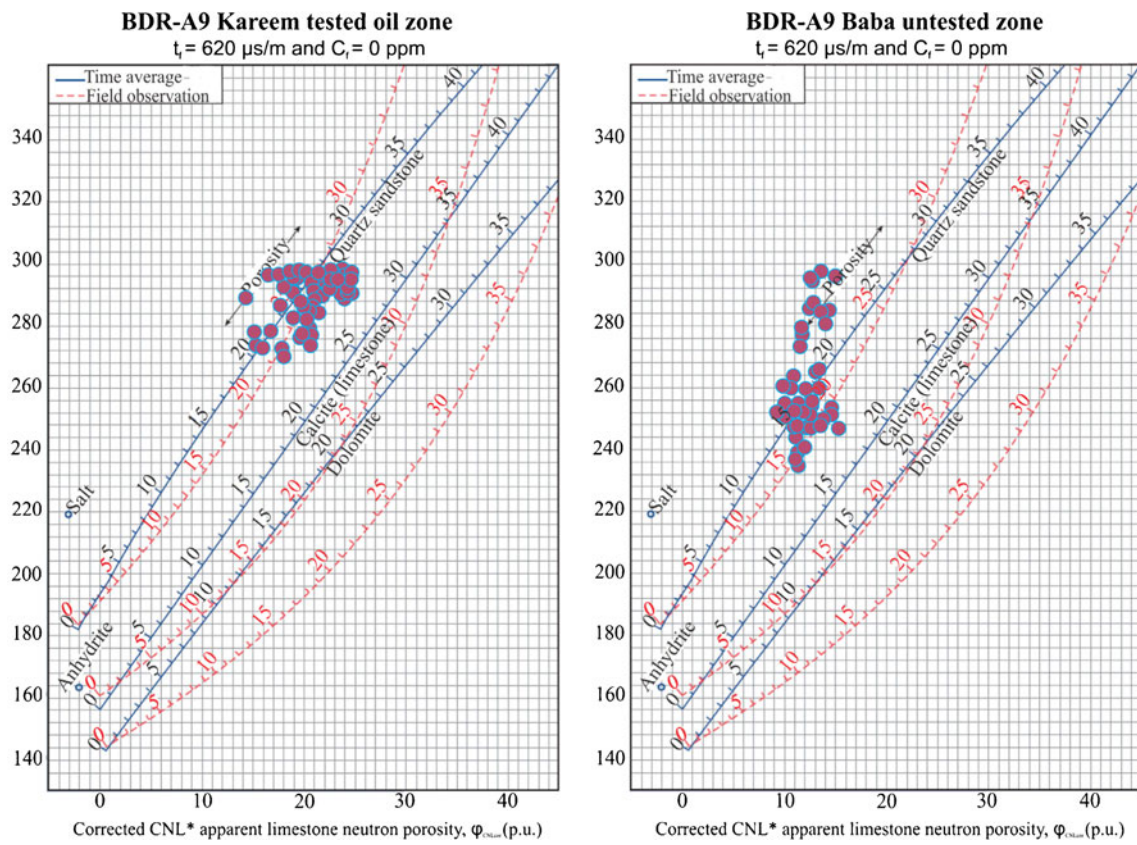


Fig. 9 Sonic-neutron crossplots of Kareem oil and water zones and Baba sand zone for BDR-A9 well

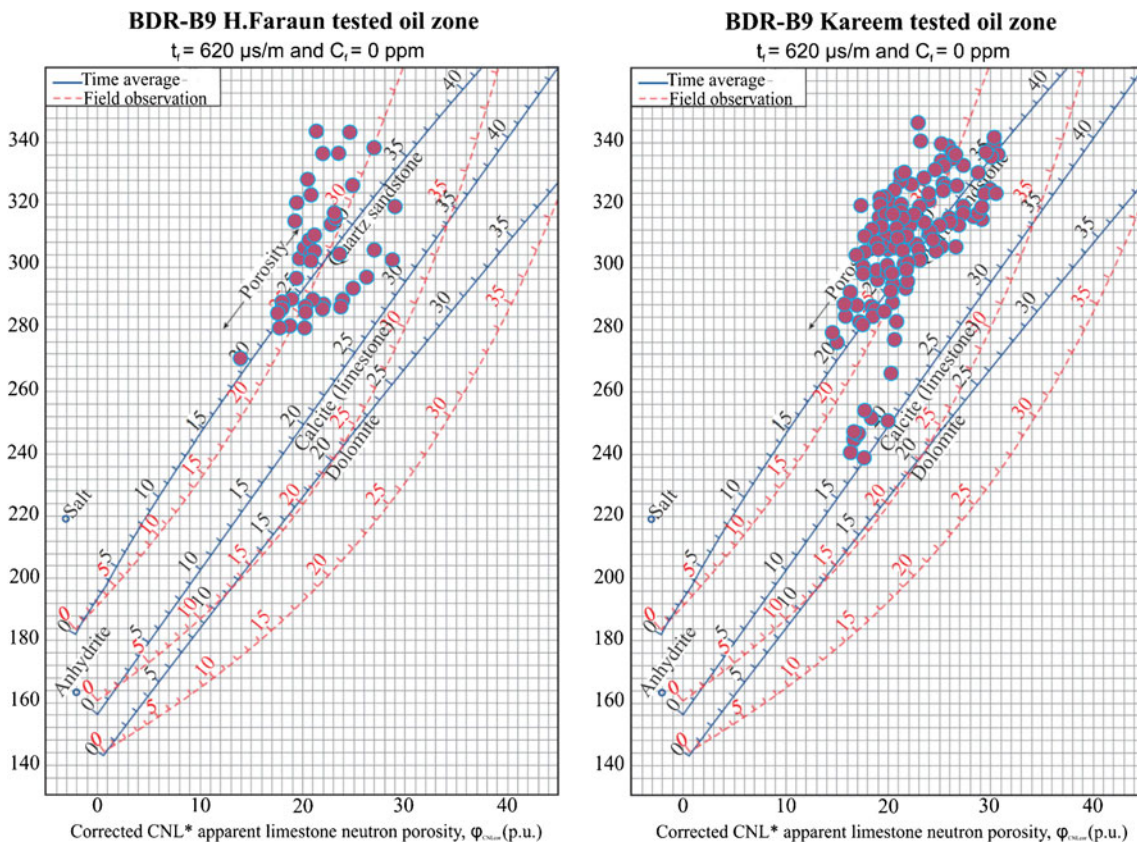


Fig. 10 Sonic-neutron crossplots of Kareem and H. Faraun S.S. oil zones for BDR-B9 well

where  $\Delta t_f$  is the sonic travel time of mud filtrate,  $\Delta t_{log}$  is the sonic log reading,  $\rho_b$  is the bulk density of the matrix,  $\rho_f$  is the fluid density,  $\phi_{nf}$  is the neutron of the fluid (100 % porosity), and  $(\phi_{nlog})$  is the neutron porosity of the matrix.

By using the *M-N* crossplot for mineral identification, the lithologic content for each horizon can be defined; matrix variations cause *M* and *N* change. Some confusion may be present due to probable shale, gas, and/or secondary porosity effects. The effect of shale shifts the points downward, while gas and secondary porosity shift the points upward. The effect of gas, shalines, secondary porosity, etc. is to shift the data points in the directions shown by the arrows (Schlumberger 1972). Different values of *M* and *N* can be plotted in the *M-N* plot and different proportions formation under investigation can be indicated in the plot depending on their matrix and fluid parameters. Finally, the actual values of *M* and *N* for common minerals and reservoir rocks are not easy to remember and have no particular significance in themselves. Although the *M-N* plot is still used, it has largely been superseded by another plot that accomplishes the same end result more elegantly.

### MID plots

It is an important technique for giving accurate results for lithological identification using charts (Schlumberger charts). The matrix identification plot (MID plot), like the *M-N* crossplot, is a crossplot technique that helps in identifying the matrix, lithology, and secondary porosity. Similar to the *M-N* crossplot, the matrix identification plot requires data from density, neutron, and sonic logs (Asquith and Krygowski 2004). The neutron and density logs are combined to define an apparent matrix density,  $(\rho_{mat})a$ . The neutron and sonic logs are combined to define an apparent matrix travel time,  $(\Delta t_{mat})a$  (Wyllie 1963).

The principle of the MID plot is similar to that of the *M-N* plot; two porosity-independent parameters—apparent matrix densities,  $(\rho_{mat})a$ , and apparent matrix sonic travel time  $(\Delta t_{mat})a$ —are crossplotted (Clavier and Rust 1976). The first step in constructing a matrix identification plot is to determine the values for the apparent matrix parameters, apparent matrix density  $(\rho_{mat})$ , and apparent matrix travel time  $(\Delta t_{mat})$ . These values are calculated from neutron  $(\phi_N)$ , density  $(\rho_b)$ , and sonic  $(\Delta t)$  data using the following equations (Atlas 1995):

$$\rho_{mat} = \rho_b - (\phi_{ND} \times \rho_n) / (1 - \phi_{ND}) \tag{3}$$

$$\Delta t_{mat} = \Delta t - (\phi_{SN} \times \rho_n) / (1 - \phi_{SN}) \tag{4}$$

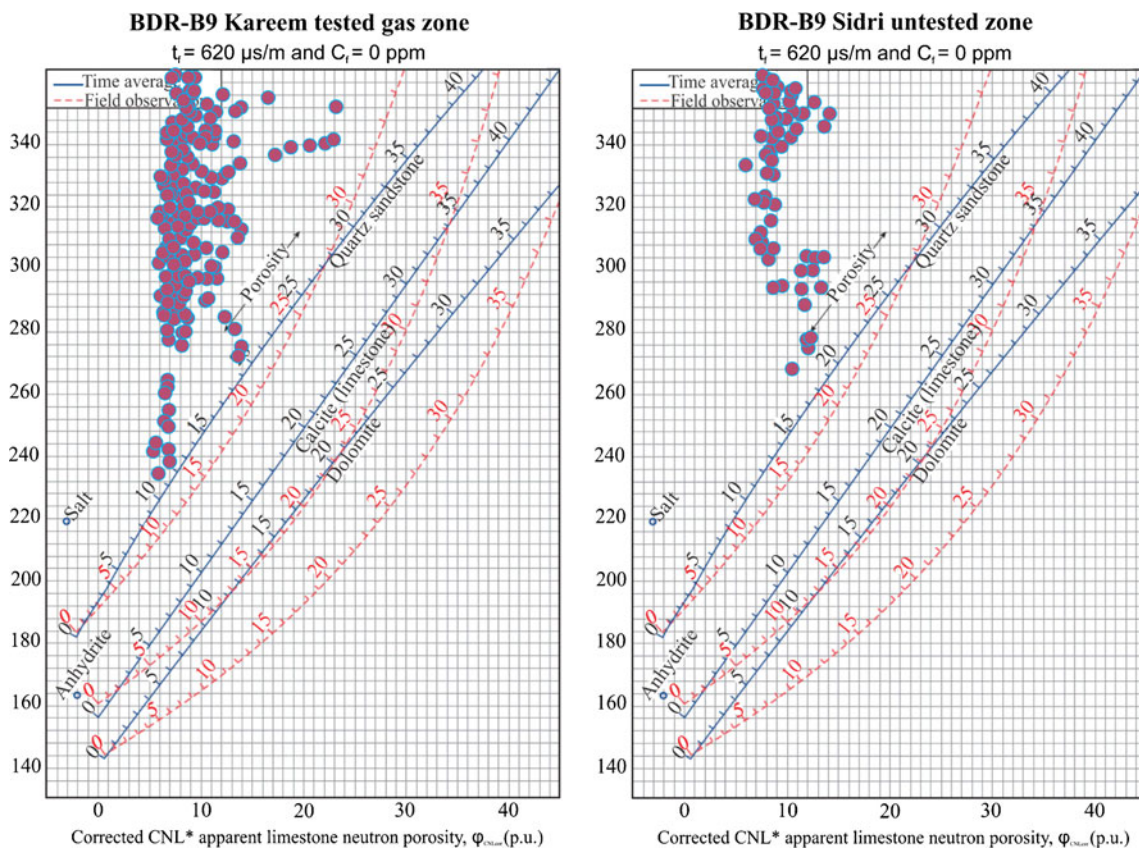


Fig. 11 Sonic-neutron crossplots of Kareem S.S. gas zone and Sidri S.S. zone for BDR-B9 well

where  $\rho_{mat}$  is the apparent grain density in grams per cubic centimeter or kilograms per cubic meter,  $\Delta t_{mat}$  is the apparent matrix interval transit time in microseconds per foot or microseconds per meter,  $\rho_b$  is bulk density from the log,  $\rho_f$  is the density of fluid,  $\Delta t$  is the interval transit time of fluid,  $\phi_{ND}$  is the neutron-density crossplot porosity, and  $\phi_{SN}$  is the sonic-neutron crossplot porosity.

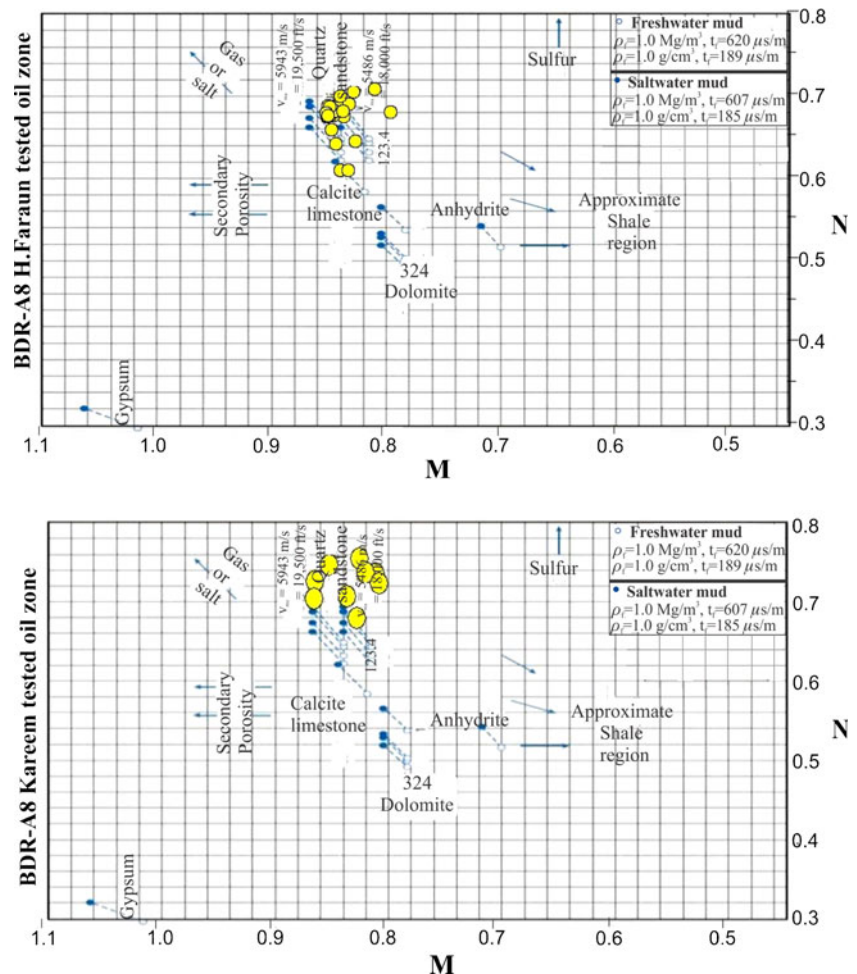
*Suggested simulation method*

Absence of pressure data in the two studied intervals leads to a search for a solution or new technique for estimating the fluid type in the studied zones.

The suggested method includes the following steps:

1. Prepare the well logging data which include the three porosity curves (density, neutron, and sonic) for the studied members and also for the tested formations which must have the same reservoir characteristics and trap mechanism.
2. Extract the well-log data for the studied members and represent it in the form of crossplots to facilitate the qualitative interpretation needed for defining the hydrocarbon effect of the studied units.
3. Plot the extracted well logging data in the two porosity measurement crossplots (density-neutron and sonic-neutron) for the produced different fluids and the untested fluids.
4. Plot the extracted well logging data in the three porosity measurement crossplots (*M-N* and MID) for the produced different fluids and the untested fluids.
5. Simulate the obtained crossplots' signatures for the untested interval with the tested oil and gas crossplots ones.
6. According to similarities and differences in the used crossplot signatures, the fluid type can be estimated for the untested units.
7. The results are recorded and then the hydrocarbon type for each used crossplot is estimated.
8. The most likely estimated hydrocarbon type for the untested studied zone is obtained when it has the same response results for all used crossplots.

**Fig. 12** *M-N* crossplots of Kareem and H. Faraun S.S. oil zones for BDR-A8 well



Mitigation of the proposed simulation method

- The three porosity logs needed in the evaluation process include density, neutron, and sonic, so two- and three-variable crossplots can be used.
- In case different hydrocarbon types result in the four used crossplot technique, another solution can be tried.
- The reservoir characteristics, the mineralogical composition, and the trap mechanism should be the same in the correlated reservoirs.

Results and discussion

In the study area, the reservoirs of Kareem, H. Faraun, Sidri, and Baba sandstones have the same trap mechanism and the same reservoir characteristics. The tested data of Kareem and H. Faraun oil and gas intervals of neutron-density, sonic-neutron, *M-N*, and MID were plotted on crossplot charts, and the results were simulated with the untested behavior of Sidri and Baba sandstone reservoirs. These correlations between the tested and the untested signatures can help in determination and confirmation of the hydrocarbon type in these reservoirs.

Schechter (2010) stated that gas affects the density-neutron crossplots, where the presence of gases in the reservoir makes the cluster go toward the northwest direction in the crossplots.

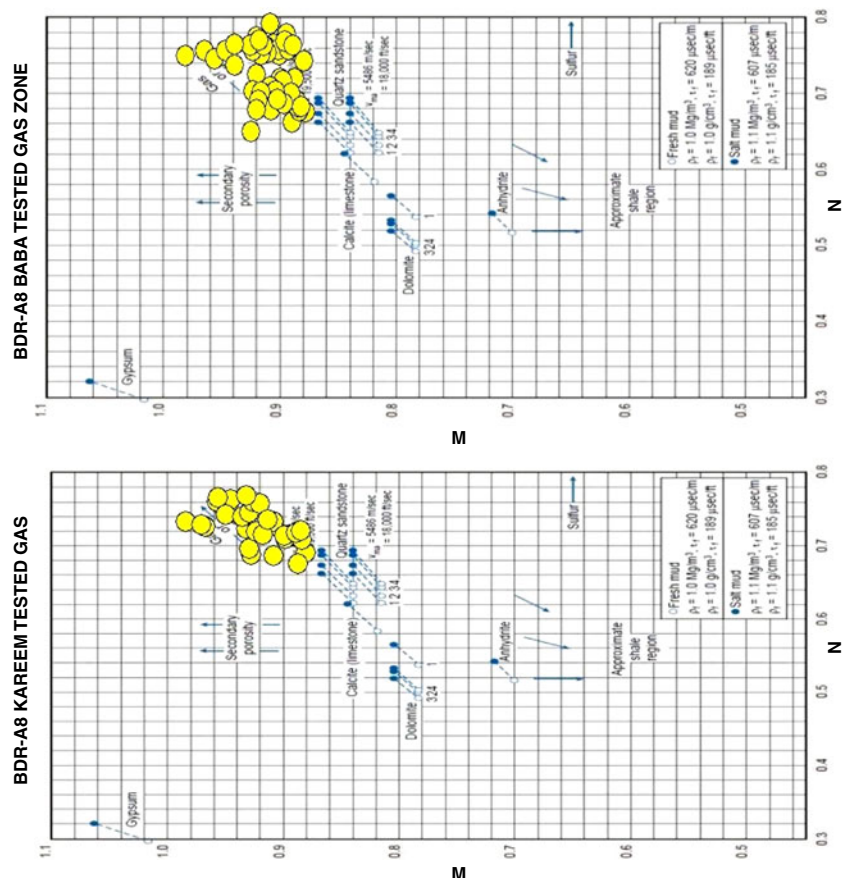
Density-neutron crossplot

Density-neutron crossplots of different reservoirs have different signatures or responses when they contain different fluid types (oil, gas, and water) (Schechter 2010). So, the correlation between neutron-density responses of different fluid types (gas, oil, and water) in Kareem Formation and H. Faraun Member intervals was undertaken with the untested Baba and Sidri reservoirs to determine their fluid type. Neutron-density crossplots were applied to all Baba and Sidri reservoir studied wells.

BDR-A8 WELL

Figure 3 represents the neutron-density crossplots of H. Faraun oil, Kareem oil, and water zones. These plots show that all of the selected zone points are plotted well in the sandstone zone, which indicates that the main lithology is sandstone. Figure 4 represents neutron-density crossplots of

Fig. 13 *M-N* crossplots of Kareem S.S. gas zone and Baba S.S. zone for BDR-A8 well



two zones (Kareem FM and Baba sandstone zone). These plots show that all of the selected points were shifted away from the sandstone zone toward the gas direction (northwest of the plot) which indicates that these zones were affected by the presence of gases. Figures 3 and 4 show the difference between neutron-density crossplot signature for (oil and gas) and they show the same response for (oil and water). The correlation of crossplot signature suggested that the Baba sandstone interval in BDR-A8 well is a gas zone.

**BDR-A9 WELL**

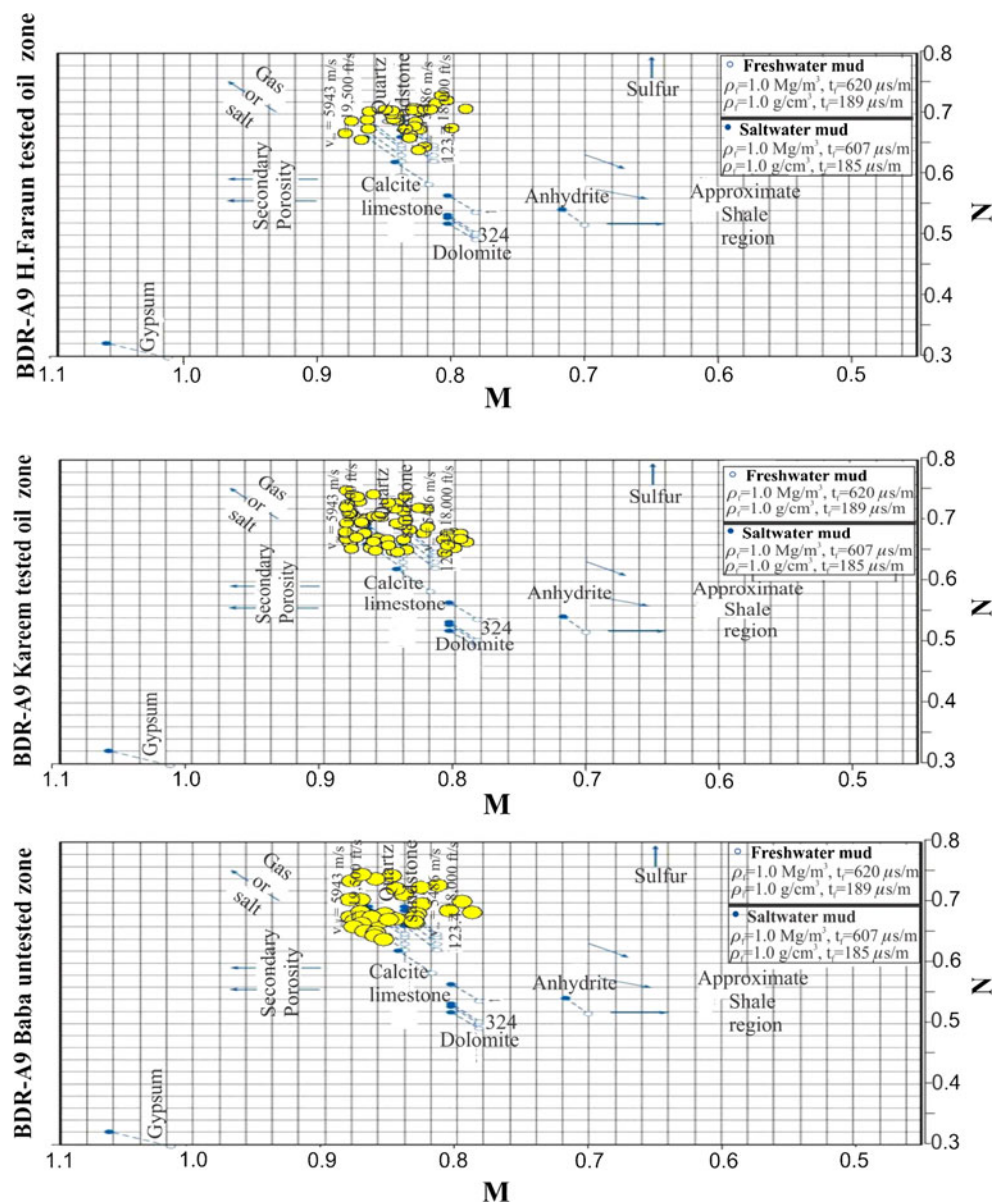
Figure 5 represents neutron-density crossplots of H. Faraun and Kareem oil zones, and Baba zone. These plots show that all of the selected zone points in these zones were plotted

exactly on the sandstone zone, which reflect that the main lithology is sandstone in these zones. The correlation revealed that there is a similarity between the neutron-density crossplots for all zones, which mean that the selected zones have the same hydrocarbon type (oil).

**BDR-B9 WELL**

Figure 6 represents neutron-density crossplots of H. Faraun and Kareem oil zones. These plots show that all of the selected zone points in these two zones were plotted well on the sandstone zone, which reflect that the main lithology is sandstone. These plots also show a similarity between the two zone responses. Figure 7 represents neutron-density crossplots of Kareem S.S. gas zone and Sidri S.S. zone. These plots shows

**Fig. 14** M-N crossplots of Kareem and H. Faraun S.S. oil zones and Baba S.S. zone for BDR-A9 well

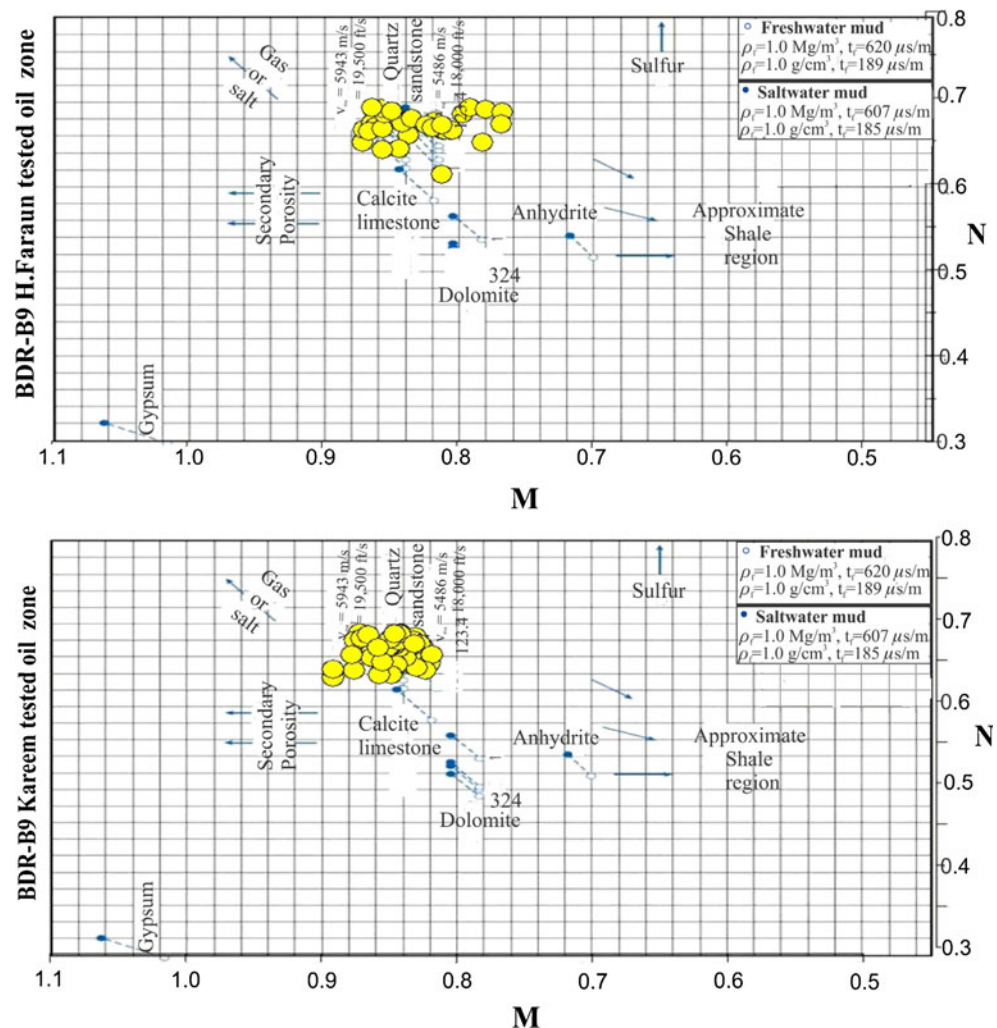


that all cluster points were shifted upward the sandstone line toward the gas direction, which indicates the presence of gases. The correlations of crossplot signatures show the similarity between Sidri S.S. zone and Kareem S.S. gas zone, so this correlation concluded that the Sidri sandstone interval in BDR-B9 well is a gas zone.

**Sonic-neutron crossplot**

The sonic-neutron crossplot can be used to differentiate between the common reservoir rock types when the clay content is negligible. It can be used to differentiate between a single known reservoir rock and the shale and to identify the evaporite minerals. Sonic-neutron crossplot technique was applied only to BDR-A8 and BDR-A9 wells because these wells have sonic logs (Schechter 2010). Gases affect the sonic-neutron crossplot, where the presence of gases makes the cluster points go toward the northwest direction in the crossplot.

**Fig. 15** M-N crossplots of plot of Kareem S.S. oil zone and Kareem S.S. water zone for BDR-B9 well



**BDR-A8 WELL**

Figure 8 represents sonic-neutron crossplots of Kareem S.S. oil, Kareem gas, and Baba S.S. zones. These plots show that all of the selected zone points in Kareem S.S. oil zone were plotted well on the sandstone zone, which reflect the sandstone lithology nature in this zone. In Baba sandstone and Kareem gas zones, the points were shifted away from the sandstone zones which indicates that these intervals were affected by the presence of gases.

The similarity between the responses of Kareem gas and Baba sandstone zones indicated that the Baba sandstone is a gas zone.

**BDR-A9 WELL**

Figure 9 represents sonic-neutron crossplots of Kareem oil and Baba sandstone zones; these plots show that all of the selected zone points in the previous zones were plotted well in the sandstone zone, but few points in Baba sandstone zone

were shifted away from the sandstone zone which were affected by the feldspar content in this interval.

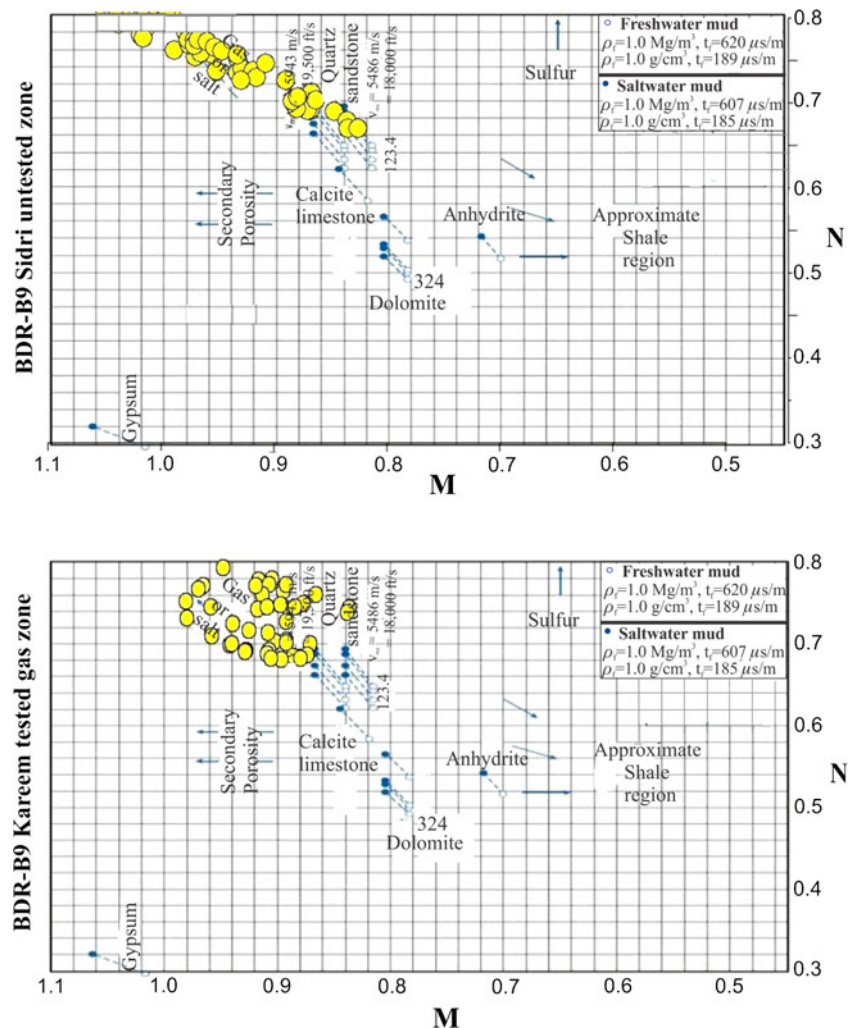
The similarity between the responses of Kareem oil zone and Baba sandstone zone proved that the Baba sandstone is an oil zone.

*BDR-B9 WELL*

Figure 10 represents sonic-neutron crossplots of H. Faraun and Kareem S.S. oil zones. These plots show that the majority of the selected zone points were plotted around the sandstone zone, which reflects the sandstone lithology nature.

Figure 11 represents sonic-neutron crossplots of the Kareem sandstone gas and Sidri sandstone zones. These plots show that the response of Sidri sandstone zone is similar to that of Kareem gas, where the majority of the Kareem gas zone and Sidri sand zone points were shifted upward away from the sandstone zone which indicates that these intervals were affected by the presence of gases.

**Fig. 16** *M-N* crossplots of Kareem S.S. gas zone and Sidri S.S. zone for BDR-B9 well



*M-N crossplot*

The *M-N* crossplot needs three porosities for *M-N* calculations, so this plot has been applied only on BDR-A8 and A9 wells. Also, the correlations between the different zones were done to help the interpretation results. This plot is useful for detection of gas zones, so the *M-N* crossplot was correlated to get the different responses in the different zones within the Baba reservoir wells.

*BDR-A8 WELL*

Figure 12 represents *M-N* crossplots of Kareem and H. Faraun sandstone oil zones. These plot show that the majority of the selected sandstone points were plotted well in the sandstone zone. They also show the lack of any effect of secondary porosity and gas effect. Figure 13 represents *M-N* crossplots of Kareem gas and Baba S.S. zones. This plot shows that the majority of the Kareem gas and Baba sand zone points were shifted upward from the sandstone zone. This indicates that these intervals were affected by the presence of gases. The



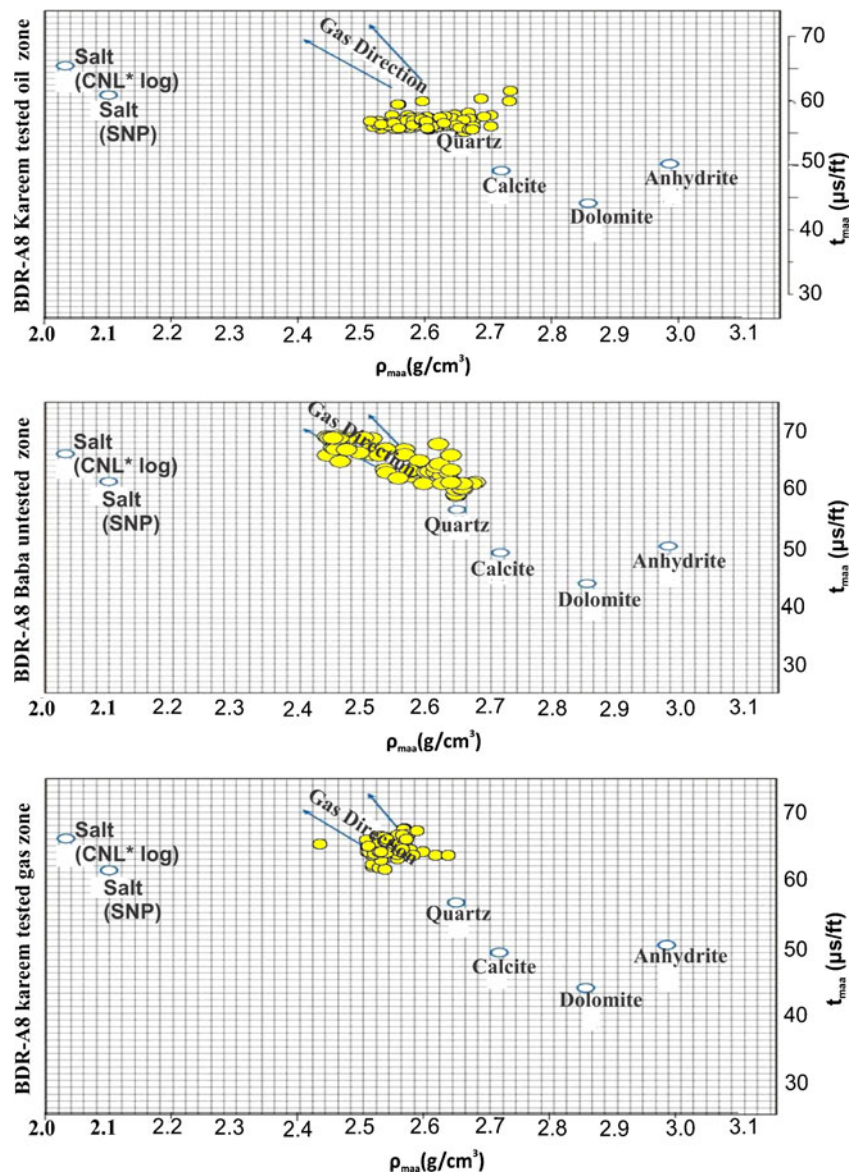
correlation between *M-N* crossplots for the different zones in BDR-A8 well shows a similarity in the responses between Kareem S.S. gas and Baba S.S. zones, which proved that the Baba S.S. zone was affected by the presence of gases.

**BDR-A9 WELL**

Figure 14 represents *M-N* crossplots of Kareem and H. Faraun S.S. oil zones, and Baba S.S. zone. These plots show that all of the selected zone points were plotted well around the sandstone zone. They also show the lack of any effect of secondary porosity and gas effect.

The similarity in *M-N* plot responses between Kareem and H. Faraun S.S. oil zones, and Baba S.S. zone, indicated that the Baba S.S. is an oil zone.

**Fig. 17** MID crossplots of Kareem S.S. oil and gas zones, and Baba S.S. zone for BDR-A8 well



**BDR-B9 WELL**

Figure 15 represents *M-N* crossplots of H. Faraun and Kareem S.S. oil zones. These plots show that the majority of the points are well plotted around the sandstone zone, except for some points which were affected by the calcareous cements and shifted to the calcite region. These plots also show the lack of any effect of secondary porosity and gas effect.

Figure 16 represents *M-N* crossplots of the Kareem gas and Sidri S.S. zones. These plots show that the majority of the Kareem gas and Sidri sand zone points were shifted upward to the gas arrow direction, which indicates that these intervals were affected by the presence of gases.

The correlation between *M-N* crossplots for the different zones in BDR-B9 well shows similarity in the responses between Kareem S.S. gas and Sidri S.S.

zones, which proved that the Sidri S.S. zone is a gas zone.

### MID crossplot

The principle of the MID crossplot is similar to that of the  $M-N$  crossplot where three porosity values are used to get values of the apparent matrix densities,  $(\rho_{mat})a$ , and the apparent matrix sonic travel time,  $(\Delta t_{mat})a$ . These values of  $(\rho_{mat})a$  and  $(\Delta t_{mat})a$  are cross plotted as shown on Figs. 17, 18, 19, and 20. This plot was applied to BDR-A8 and BDR-A9 wells only. Also, it was correlated between different zones to validate the interpretation results.

#### BDR-A8 WELL

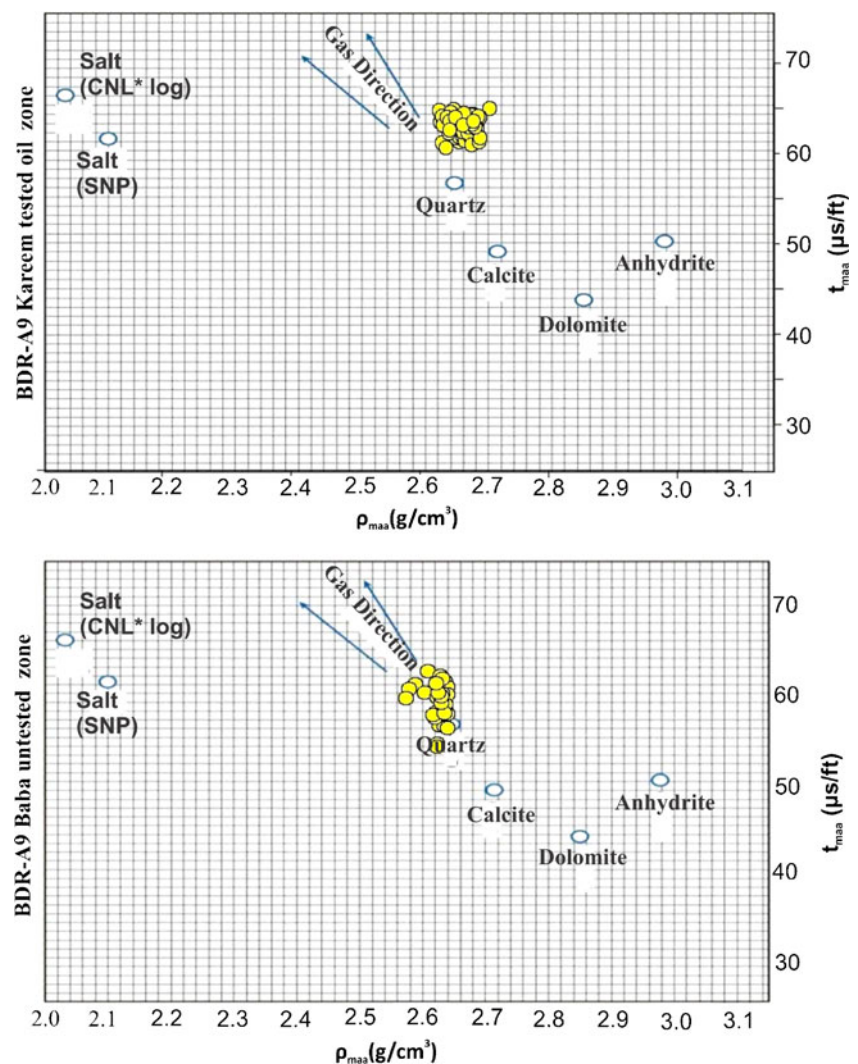
Figure 17 represents the MID plot of Kareem S.S. oil, Kareem S.S. gas, and Baba S.S. zones. The Kareem S.S. oil zone plot shows that all of the selected zone points were well plotted on

the sandstone zone, which indicated that the main lithology is sandstone and there is no gas effect. But, the Kareem S.S. gas zone and Baba S.S. zone plots show that the entire selected zone points were plotted upward the sandstone zone, and concentrated between the gas direction arrows, which indicated the gas effect. The similarity in MID plot responses between Kareem S.S. gas and Baba S.S. zones indicated that the Baba S.S. zone is a gas zone.

#### BDR-A9 WELL

Figure 18 represents the MID plot of Kareem S.S. oil and Baba S.S. zones. These plots showed that all the selected zone points are plotted around the sandstone zone, which indicated that the main lithology is sandstone and there is no gas effect. The average matrix transit time  $(\Delta t_{mat})a$  of Baba sandstone Member is  $60 \mu\text{s}/\text{ft}$  while the average matrix density  $(\rho_{mat})a$  is  $2.60 \text{ g}/\text{cc} \mu\text{s}/\text{ft}$ . The similarity in MID plot response

**Fig. 18** MID crossplots of Kareem S.S. oil zone and Baba S.S. zone for BDR-A9 well



between Kareem S.S. oil and Baba S.S. zones concluded that the Baba S.S. zone is an oil zone.

**BDR-B9 WELL**

Figure 19 represents the MID plot of Kareem and H. Faraun S.S. oil zones. These plots show that all of the zone points are well plotted around the sandstone region, which indicates that the main lithology is sandstone. These plots show the lack of any effect of secondary porosity and gas effect. Figure 20 represents the MID plots of Kareem S.S. gas and Sidri S.S. zones. They show that all of the selected zone points are plotted upward the sandstone zone and concentrated between the gas direction arrows, which indicate that the gas effect shifted points to the gas direction zone. Figures 19 and 20 show the similarity between the Kareem S.S. gas and Sidri S.S. zones, which confirms the gas effect in Sidri S.S. zone. Also, these plots show the difference between gas-bearing zones (Kareem and Sidri sandstones) and the oil-bearing zones (Kareem and H. Faraun sandstones). The average matrix transit time

$(\Delta t_{mat})a$  of Sidri sandstone is 65  $\mu\text{s}/\text{ft}$ , while the average matrix density  $(\rho_{mat})a$  is 2.47  $\text{g}/\text{cc}$   $\mu\text{s}/\text{ft}$ . The similarity in MID plot response between Kareem S.S. gas zone and Sidri S.S. zone suggested that Sidri S.S. zone is a gas zone.

All results of the simulation technique are summarized in Table 1.

**Conclusions**

This study revealed that use of the suggested systematic crossplot simulation method shows good results in the estimation of the hydrocarbon type in the absence of pressure data, which helps to estimate the most likely estimated hydrocarbon type in the untested studied (S.S.) zones of Sidri and Baba members.

The two-variable (neutron-density, sonic-neutron) crossplots and the three-variable petrophysical techniques (*M-N* and MID) crossplots were applied on the tested oil and gas zones in BDR-A8, A9, and B9 wells and simulated with

**Fig. 19** MID crossplots of Kareem and H. Faraun S.S. oil zones for BDR-B9 well

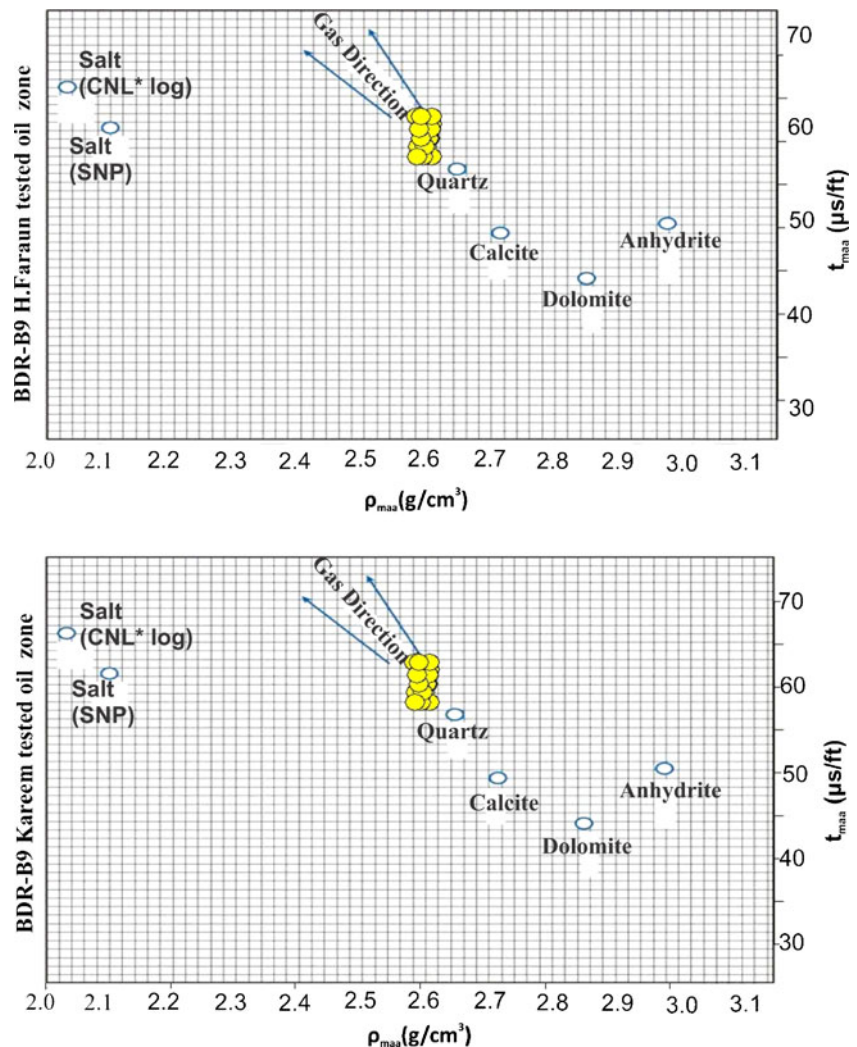
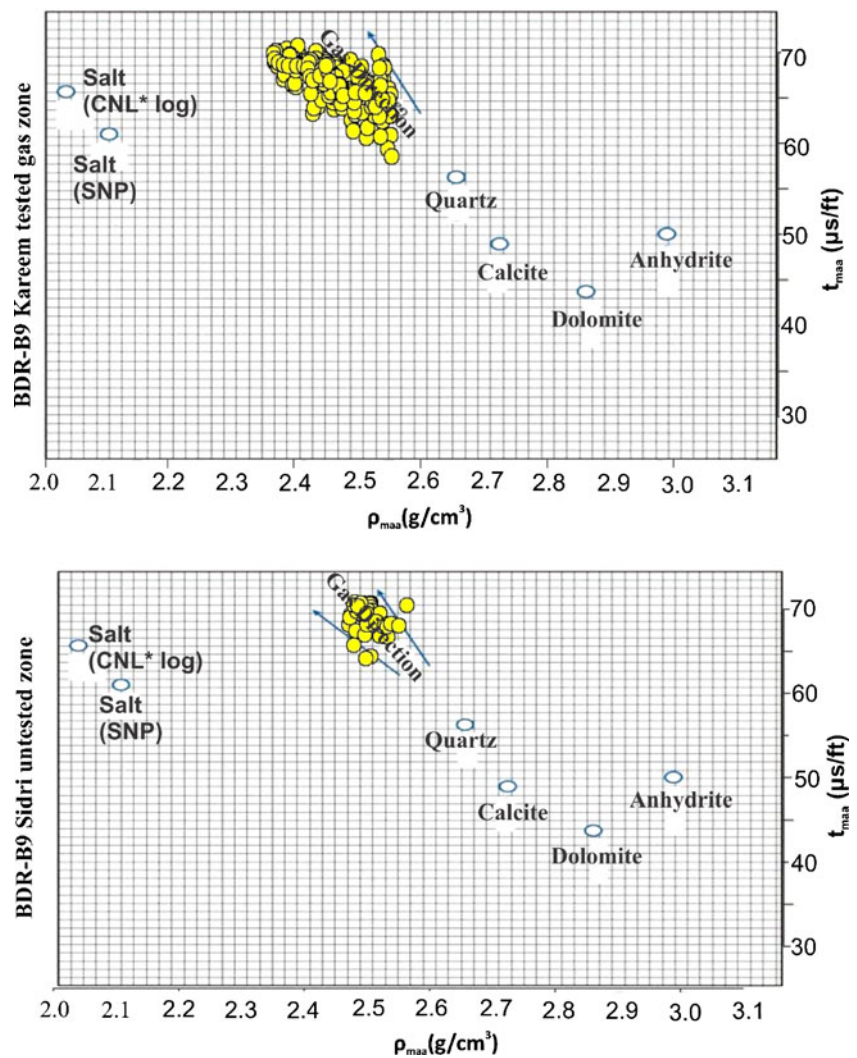


**Fig. 20** MID crossplots of Kareem S.S. gas zone and Sidri S.S. zone for BDR-B9 well



the untested interval crossplot signature; the results of the applied petrophysical techniques were as follows:

- The neutron-density crossplot correlation indicated that the Baba sandstone zone signature is very similar with the tested gas zone in H. Faraun Member and Kareem FM, which indicates a gas zone in BDR-A8 well and an oil zone in BDR-A9 well at the level of Baba S.S. reservoir. The correlation shows similarity in signature between the tested gas zone in H. Faraun Member and

Kareem Formation in BDR-B9 well at the level of Baba S.S. reservoir.

- The sonic-neutron crossplot simulation indicated that the Baba sandstone zone is a gas zone in BDR-A8 well, and it is an oil zone in BDR-A9 well. Also, it indicated that Sidri sandstone zone is a gas zone in BDR-B9 well.
- The tri-porosity (*M-N*) crossplot correlation indicated that Baba sandstone zone is a gas zone in BDR-A8 well, while it is an oil zone in BDR-A9 well. Also, it indicated that the Sidri sandstone zone is a gas zone in BDR-B9 well.

**Table 1** Final results of hydrocarbon type for Baba and Sidri sandstone zones in the studied wells

Well name	Member name	Final estimated fluid type from crossplots				Final results
		Neutron-density	Neutron-sonic	<i>M-N</i>	MID	
BDR-A8	Baba	Gas	Gas	Gas	Gas	Gas
BDR-A9	Baba	Oil	Oil	Oil	Oil	Oil
BDR-B9	Sidri	Gas	Gas	Gas	Gas	Gas

The MID crossplot simulation indicated that the Baba sandstone zone is a gas zone in BDR-A8 well, while it is an oil zone in BDR-A9. Also, it indicated that Sidri sandstone zone is a gas zone in BDR-B9 well.

The final results of the suggested simulation method concluded that:

1. The hydrocarbon type is gas in Baba (S.S.) zone for the BDR-A8 well and Sidri (S.S.) zone for the BDR-B9 well, and an oil zone for Baba (S.S.) zone for the BDR-A9 well.
2. The BDR-A8 well is a gas well, while BDR-A9 is an oil well in the level of Baba sandstone zone.
3. The BDR-B9 well is a gas-bearing well, on the level of Sidri sandstone zone.

### Recommendations

From the previously mentioned findings, the following recommendations should be noteworthy:

1. Use this suggested simulation method in case of the absence of the pressure data to estimate the hydrocarbon type
2. Perform repeated formation test (RFT) against the studied zones to know the reservoir pressure
3. Perforate the untested Baba (S.S.) interval in BDR-A8 well and the untested Sidri (S.S.) interval in BDR-B9 well, which was proven as a gas zone, and the untested Baba (S.S.) interval in BDR-A9 well as oil zone.

**Acknowledgments** The authors are grateful to the two reviewers and the editor for the time and the effort they put into their comments that helped improve this paper. The authors express their kind thanks to Prof. Dr. Hussein M. A. Alkhashab, Professor of Applied Geophysics, for his valuable comments to revise this manuscript. Also, deep thanks to the EGPC and GUPCO authorities for their permission to carry out this research and providing the required data. The authors thank the production team of Springer for their efforts to improve the quality of this paper.

### References

- Alsharhan A, Salah M (1994) Geology and hydrocarbon habitat in a rift setting: southern Gulf of Suez. *Egypt Bull Can Petrol Geol* 42:312–331
- Asquith G, Krygowski D (2004) Basic well log analysis: AAPG methods in exploration. *Am Assoc Pet Geol Bull, Oklahoma* 16:31–35
- Atlas W (1995) Introduction to wireline log analysis. Western Atlas International Inc, Houston, Texas
- Bosworth W, McClay K (2001) Structural and stratigraphic evolution of the Gulf of Suez Rift, Egypt: a synthesis. In P.A. Ziegler, W. Cavazza, A.H.F. Robertson and S. Crasquin-Soleau (Eds.), *Peri-Tethys Memoir 6: Peri-Tethyan rift/wrench basins and passive margins*. *Me'moires du Museum National d'Histoire naturelle de Paris, Memoir* 186:567–606
- Clavier C, Rust DH (1976) Mid-plot, a new lithology technique. *Log Anal* 17:16–31
- El-Naby AA, El-Aal MA, Kuss J, Boukhary M, Lashin A (2009) Structural and basin evolution in Miocene time, southwestern Gulf of Suez. *Egypt Neues Jahrbuch für Geologie und Paläontologie-Abhandlungen* 251:331–353
- El-Naby A, Ghanem H, Boukhary M, El-Aal MA, Lüning S, Kuss J (2010) Sequence-stratigraphic interpretation of structurally controlled deposition: Middle Miocene Kareem Formation, southwestern Gulf of Suez. *Egypt Egypt: GeoArabia* 15:129–150
- Lashin A, Abd El-Aal M (2004) Seismic data analysis to detect the depositional process environments and structural framework of the east central part of Gharib Province, Gulf of Suez-Egypt. *Ann Egypt Geol Surv* 27:523–550
- Pirson JS (1977) *Geologic well log analysis*. Gulf Publishing Company, Amsterdam, New York, pp 407–411
- Said R (1990) Cretaceous paleogeographic maps. In: Said R (ed) *The geology of Egypt*. A A Balkema, Rotterdam, pp 439–449
- Schechter D (2010) Crossplot. Porosity and lithology, Formation evaluation pete., p 321
- Schlumberger (1972) *Log interpretation principles*, vol 1. Schlumberger Limited, New York, USA, p 112
- Schlumberger (1986) *Well evaluation conference* Schlumberger Ltd., pp 1–31
- Schlumberger (1987) *Log interpretation principles/applications*. Schlumberger Company Publication, Houston, Texas, pp 3–10, ISBN: SMP-7017
- Schlumberger (1995) *Well evaluation conference—Egypt*. Houston, Texas pp 1–87
- Schlumberger (1997) *Log interpretation charts*. Schlumberger Ltd Houston, Texas, pp 72175–77252
- Wyllie MRJ (1963) *The fundamentals of well log interpretation*. New York, Academic Press